DOE/NASA/16310-7
NASA TM-101446

Tensile Behavior of Tungsten and Tungsten-Alloy Wires from 1300 to 1600 K

Hee Mann Yun
National Aeronautics and Space Administration
Lewis Research Center

Work performed for
U.S. DEPARTMENT OF ENERGY
Nuclear Energy
Reactor Systems Development and Technology

Prepared for
The Metallurgical Society Fall Meeting
cosponsored by The Metallurgical Society of AIME and the
American Society for Metals
Chicago, Illinois, September 27-29, 1988

DISCLAIMER

Printed in the United States of America

Available from
National Technical Information Service
U.S. Department of Commerce
5285 Port Royal Road
Springfield, VA 22161

NTIS price codes[1]
Printed copy: A02
Microfiche copy: A01

[1]Codes are used for pricing all publications. The code is determined by the number of pages in the publication. Information pertaining to the pricing codes can be found in the current issues of the following publications, which are generally available in most libraries: *Energy Research Abstracts (ERA); Government Reports Announcements* and Index (*GRA* and I); *Scientific and Technical Abstract Reports (STAR);* and publication, NTIS-PR-360 available from NTIS at the above address.

TENSILE BEHAVIOR OF TUNGSTEN AND TUNGSTEN-ALLOY WIRES FROM 1300 TO 1600 K

Hee Mann Yun*

National Aeronautics and Space Administration
Lewis Research Center
Cleveland, Ohio 44135

Summary

The tensile behavior of 200-μm-diameter tungsten lamp (218CS-W), tungsten + 1.0 atomic percent (a/o) thoria (ST300-W), and tungsten + 0.4 a/o hafnium carbide (WHfC) wires was determined over the temperature range 1300 to 1600 K at strain rates of 3.3×10^{-2} to 3.3×10^{-5} sec^{-1}. Although most tests were conducted on as-drawn materials, one series of tests was undertaken on ST300-W wires in four different conditions: as-drawn and vacuum annealed at 1535 K for 1 hr, with and without electropolishing. Whereas heat treatment had no effect on tensile properties, electropolishing significantly increased both the proportional limit and ductility, but not the ultimate tensile strength. Comparison of the behavior of the three alloys indicates that the HfC-dispersed material possesses superior tensile properties. Theoretical calculations indicate that the strength/ductility advantage of WHfC is due to the resistance to recrystallization imparted by the dispersoid.

---

*National Research Council - NASA Research Associate. NASA Lewis Research Center, Cleveland, Ohio 44135.

Introduction

In high temperature metal matrix composites, the reinforcing fiber carries the preponderance of the applied load; thus tungsten alloys have typically been chosen as the preferred fiber because of their great strength and stiffness at temperatures greater than 1300 K. In the past, high-temperature tensile and creep behavior (1,2) of as-drawn tungsten and tungsten-alloy wires have been studied. Their properties were attributed to potassium dopants (3), in the case of lamp grade tungsten (218CS-W) or thoria dispersoids (4) (ST300-W), as well as heavily drawn fibrous microstructures. In the present study the tensile properties of current commercial and experimental tungsten-alloy wires are examined over the temperature range 1300 to 1600 K (homologous temperature ranging from 0.4 to 0.5) as a function of strain rate. In addition, both as-drawn (cold worked) and annealed thoria-strengthened alloy wires were tested with and without an electropolished surface in order to determine the effect of processing on mechanical properties.

Experimental Procedure

Materials

Table I shows chemical compositions of the three tungsten-alloy wires examined in this work. The tungsten alloys 218CS-W (strengthened with potassium bubbles) and ST300-W (thoria-strengthened) were commercially available, whereas the HfC-strengthened material was an experimental alloy. In all cases the alloy wires were fabricated by powder metallurgy techniques and drawn to their final nominal diameter of 0.2 mm. The fibrous grain structure of these three materials is illustrated in Fig. 1. The ST300-W wires were examined both in the as-drawn condition and after a 1 hr vacuum stress relief anneal at 1535 K (Fig. 2(a)) which is typical of the processing heat treatments utilized to fabricate metal matrix composites (5). In addition, specimens electropolished in a 1 n NaOH solution at 9V for 30 sec with the wire being rotated at about 1 revolution/sec (6) were tested. Polishing reduced the specimen diameter to 0.14 mm with a mean deviation of 0.01 mm along the approximately 25.4-mm-long electropolished zone.

Table I. - Chemical Composition of 218CS-W, ST300-W, and WHfC Wires

Material	Chemical composition, a/o				
	C	Hf	ThO_2	K	W
ST300-W	----	----	1.0	-----	Balance
WHfC	0.44	0.41	---	-----	Balance
218CS-W	----	----	---	0.038	Balance

Mechanical Property Test Procedures

Tensile testing was conducted in a vacuum of 10^{-4} Pa at temperatures ranging from 1300 to 1600 K. Tensile properties were determined at constant cross-head speeds ranging from 0.00085 to 0.85 mm/sec; furthermore, all tensile strength properties were determined from the autographically recorded load - time curves. Because the wire specimens were mechanically

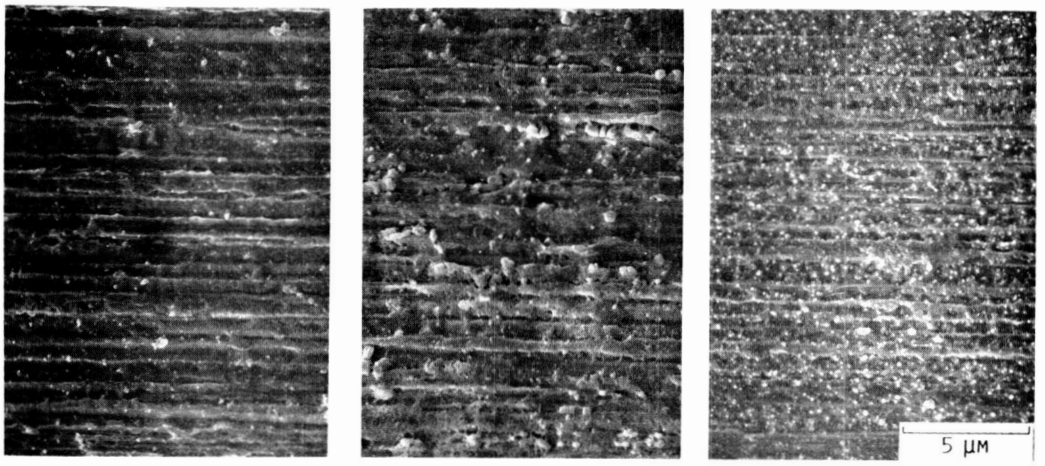

Figure 1. - Scanning electron microscope photomicrographs of as-drawn tungsten alloy wires, prior to tensile testing (longitudinally sectioned and etched), of a) 218CS-W, b) ST300-W, and c) WHfC.

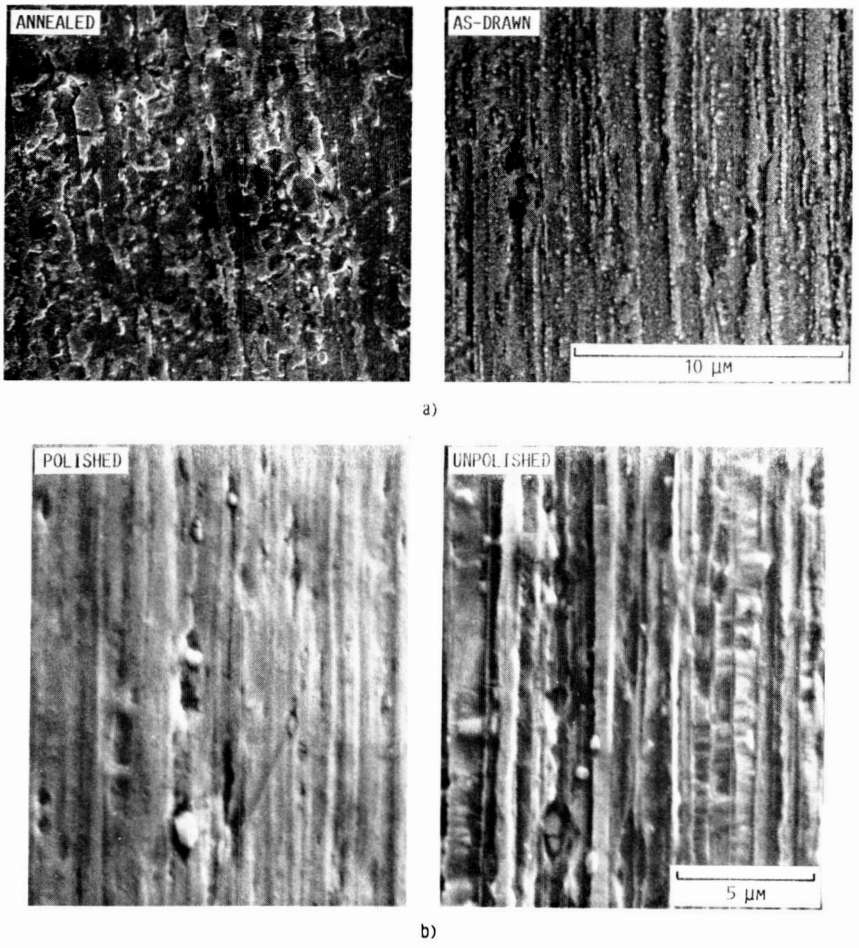

Figure 2. - Scanning electron microscope photomicrographs of a) as-drawn and vacuum-annealed (for 1 hr at 1535 K) ST300-W wires, longitudinally sectioned and etched, and b) polished and unpolished surfaces of as-drawn ST300-W wires (all made prior to tensile testing).

gripped outside the hot zone of the furnace, the gauge length was not known; hence the data were analyzed under gauge-length-independent conditions (i.e., only the proportional limit, ultimate tensile strength, and reduction of area were determined). Tensile tests of electropolished samples were evaluated with the assumption that the deformation was taking place only in the reduced diameter gauge section zone. This supposition was reasonable, as shown by several tests measuring elongation of electropolished specimens by optical tracking with a cathetometer. These tests were conducted at the slowest velocity--an initial strain rate of 3.3×10^{-5} sec^{-1}. Good agreement was found between strain rates calculated from extension - time data, $(2.5 \pm 0.5) \times 10^{-5}$ sec^{-1}, and cross-head motion - time data, $(3.3 \pm 0.3) \times 10^{-5}$ sec^{-1}.

Microstructural Examination

The longitudinal grain structure of as-received, heat-treated, electropolished, and tested wires was studied with both light optical and scanning electron microscope (SEM) techniques.

Results

Influence of Surface Finish and Annealing on ST300-W

Typical tensile properties of the ST300-W wire, including proportional limit (PL), ultimate tensile strength (UTS), and reduction of area (RA) are shown in Fig. 3 as functions of temperature, surface condition, and heat treatment for materials tested at a constant cross-head speed of 0.0085 mm/sec (approximate strain rate of 3.3×10^{-4} sec^{-1}). Both strength (Fig. 3(a)) and ductility (Fig. 3(b)) generally decrease with increasing temperature. Although the elevated temperature UTS is essentially independent of surface finish and/or heat treatment, electropolishing has clearly improved the PL and RA. The 1535 K anneal for 1 hr appears to have no effect. The higher PL and RA of the electropolished specimens, compared to the as-drawn samples, are probably due to the elimination of surface flaws which cause (1) premature yielding by local reduction of the cross-sectional area and (2) premature fracture by joining the surface defects with internal cracks.

The microstructural difference between as-drawn and annealed ST300-W wire (Fig. 2(a)) was slight; namely (1) a partial destruction of the fibrous structure and (2) a slight increase in the width of the grains. The anneal can, therefore, be characterized as a stress relief heat treatment wherein the grain and subgrain structure remain essentially unchanged. This behavior is in agreement with Tajime's (7) view that complete recovery in tungsten wires can only begin to take place above 1573 K. Therefore, it can be concluded that the heat treatment at 1535 K does not cause any strength or ductility decrease in the temperature range from 1300 to 1600 K.

Tensile Properties

The influence of alloy chemistry on the PL and UTS is shown in Fig. 4 where these properties are plotted as a function of temperature for materials tested at a constant cross-head speed of 0.0085 mm/sec (approximate strain rate of 3.3×10^{-4} sec^{-1}). From 1300 to 1600 K, the hafnium carbide-dispersed WHfC wires consistently displayed higher PL's (Fig. 4(a)) than either the thoria- or potassium bubble-dispersed wires. Below 1500 K the thoria-dispersed ST300-W possessed higher yield strengths

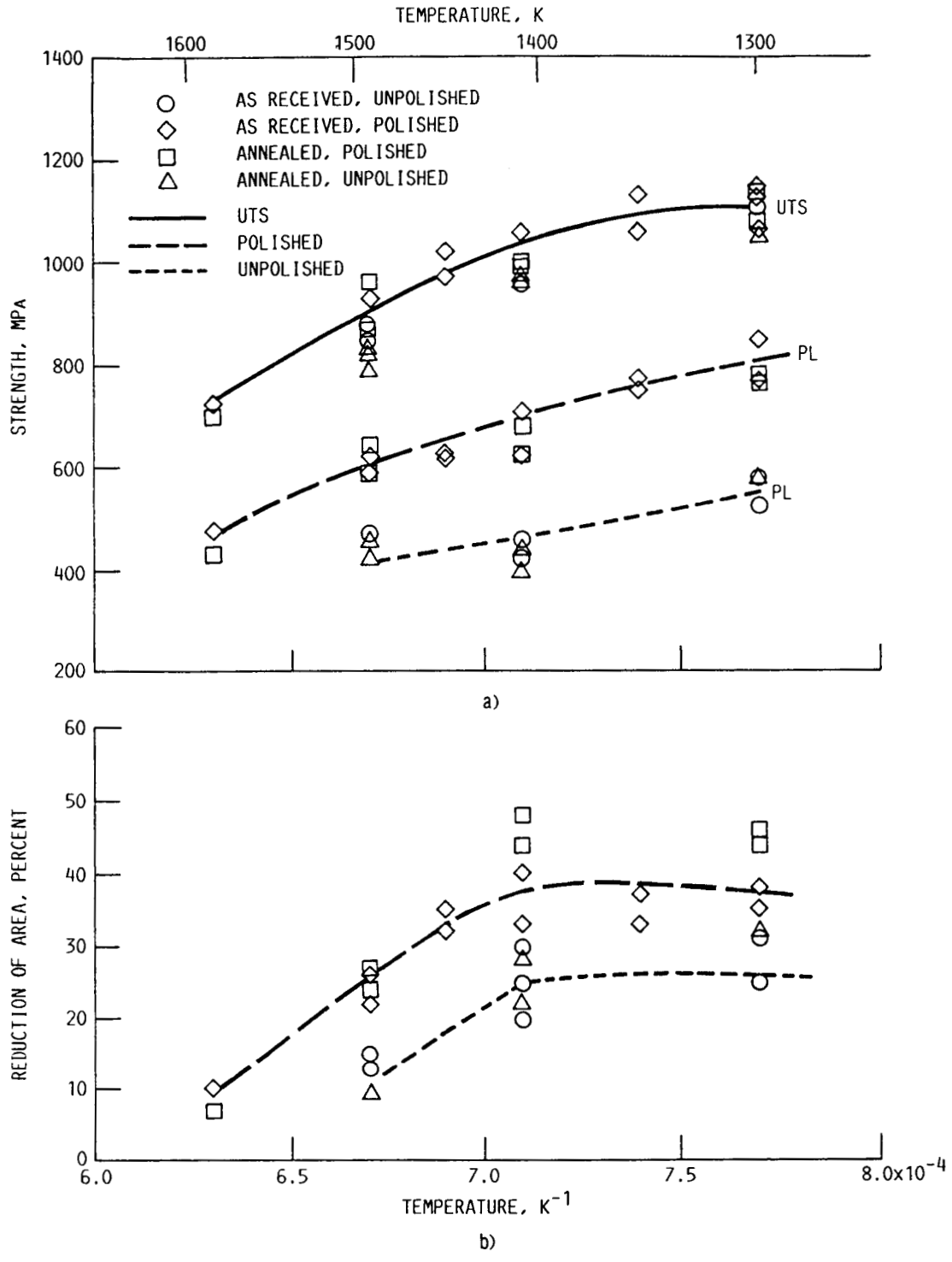

Figure 3. - Effect of surface condition and a 1-hr vacuum anneal at 1535 K on a) ultimate tensile strength and proportional limit and b) reduction of area for ST300-W wires tested at 0.0085 mm/sec (estimated initial strain rate = 3.3×10^{-4} sec^{-1}).

than potassium bubble-dispersed wires; however, with increasing temperature the difference in yield strengths becomes small. In terms of ultimate tensile strength, the WHfC wire has a considerable strength advantage over the 218CS-W or ST300-W at the higher test temperatures (Fig. 4(b)). However, at 1300 K the strength of WHfC and ST300-W are similar, and the potassium bubble-strengthened wire 218CS-W is much weaker.

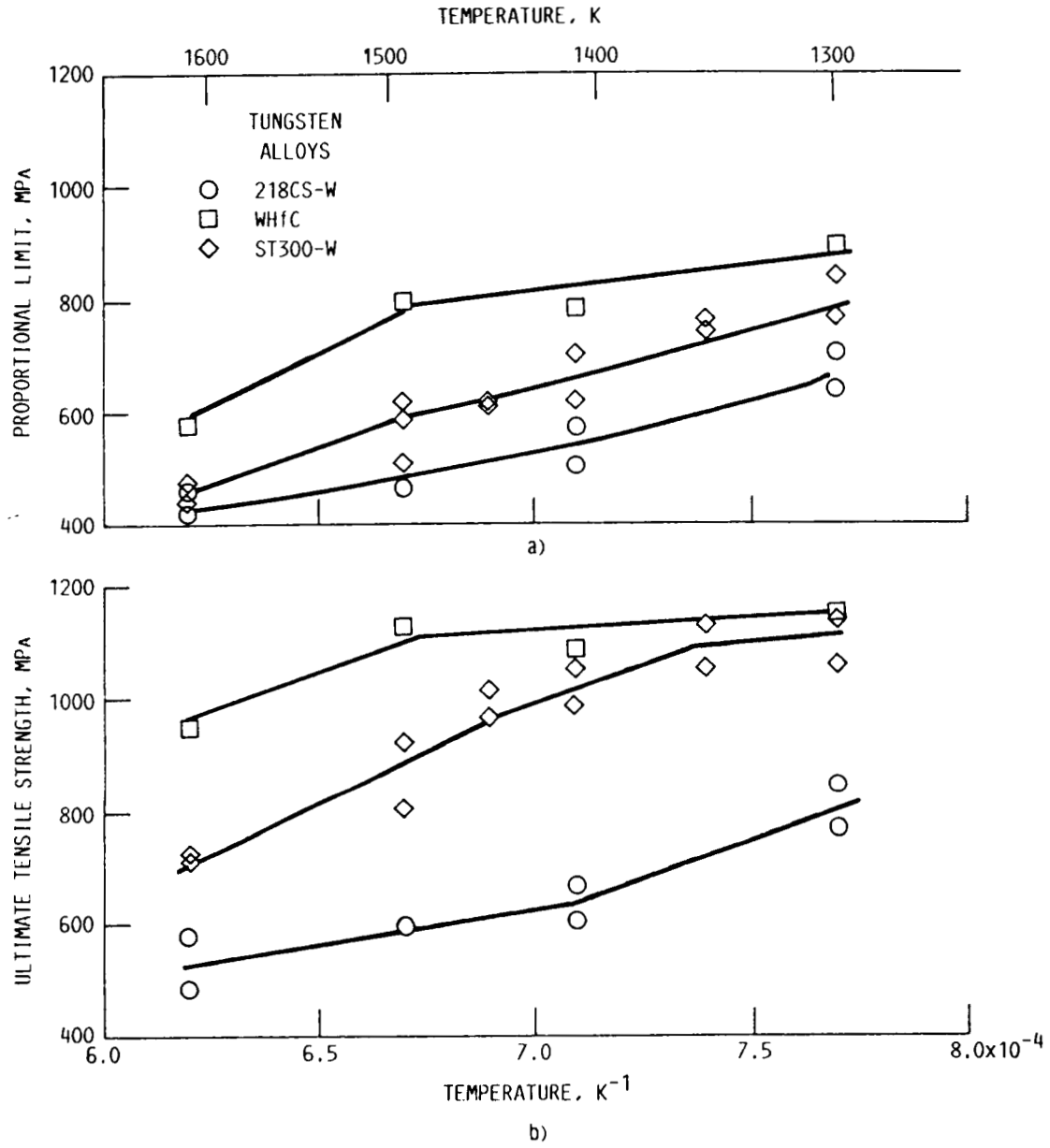

Figure 4. - a) proportional limit and b) ultimate tensile strength of tungsten-alloy wires tested at 0.0085 mm/sec.

Stress - Strain Rate Behavior

The effect of strain rate on the PL and RA is shown in Figs. 5 and 6, respectively, for as-drawn, electropolished wires at 1400 and 1600 K. The measure of yield strength is relatively constant over two to three orders of magnitude of strain rate for WHfC wires at 1400 K (Fig. 5(a)) and for ST300-W and 218CS-W at 1600 K for fast strain rates (Fig. 5(b)). Conversely, the PL's gradually decrease for WHfC wires at 1600 K (Fig. 5(b)) and ST300-W and 218CS-W wires at 1400 K (Fig. 5(a)) as the strain rate is decreased from 0.033 to 0.000033 sec^{-1}. By following normal convention, the data in Fig. 5 have been analyzed in terms of the power law deformation behavior,

$$\dot{\varepsilon} = A\sigma^n \tag{1}$$

$$\sigma = B\dot{\varepsilon}^m \tag{2}$$

where $\dot{\varepsilon}$ and σ are the strain rate and stress (PL in this work), respectively, n is the stress exponent, and m is the strain rate sensitivity with $n = 1/m$. Table II summarizes the calculated strain rate sensitivities as functions of temperature, strain rate range, and alloy composition. Warren et al. (2) reported n = 7 to 8 (m = 0.13 to 0.14) for ST300-W-like thoria-dispersed tungsten wires tested at 1400 K and a strain rate of 10^{-8} sec^{-1}. This is somewhat different from m = 0.086 (n = 11.5), determined for ST300-W at 1400 K and strain rates less than 10^{-3} sec^{-1}. The different stress exponent would be caused from the different strain rate region.

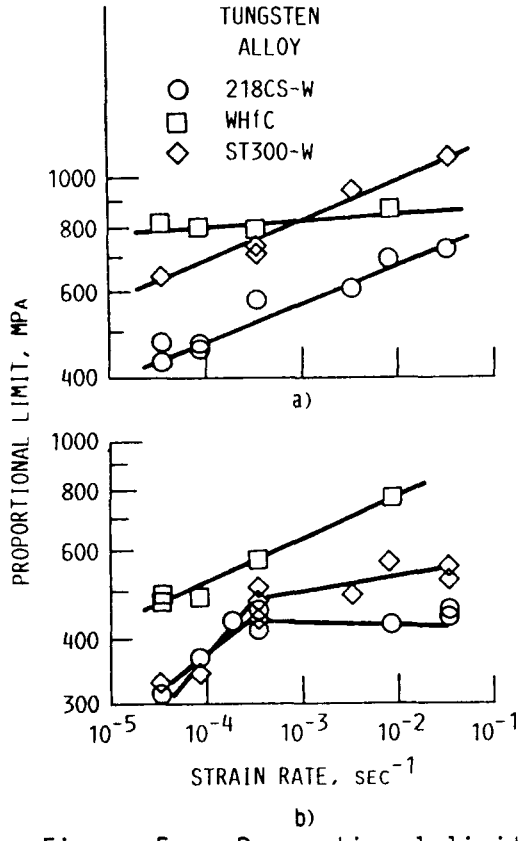

Figure 5. - Proportional limit at a) 1400 K and b) 1600 K as a function of initial strain rate for several tungsten-alloy wires.

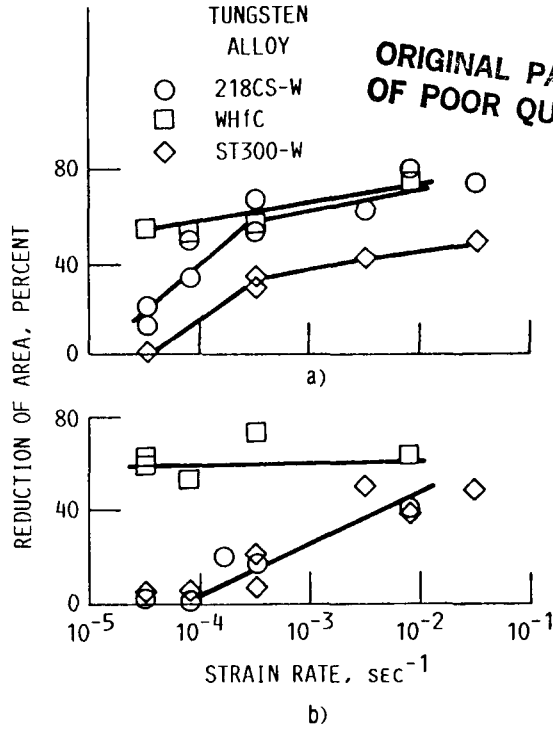

Figure 6. - Reduction of area at a) 1400 K and b) 1600 K as a function of initial strain rate for several tungsten-alloy wires.

Table II. - Strain Rate Sensitivities of Various W-Alloy Wires

Material (dispersoid)	Temperature, K	Strain rate sensitivity, m	Strain rate range, sec^{-1}
ST300-W (thoria)	1400	0.086	$3x10^{-5}$ to $3x10^{-2}$
	1600	.19	$3x10^{-5}$ to $1x10^{-3}$
	1600	.039	$1x10^{-3}$ to $3x10^{-2}$
218CS (bubbles)	1400	.086	$3x10^{-5}$ to $3x10^{-2}$
	1600	.15	$3x10^{-5}$ to $1x10^{-3}$
	1600	.001	$1x10^{-3}$ to $3x10^{-2}$
WHfC (HfC)	1400	.014	$3x10^{-5}$ to $3x10^{-2}$
	1600	.091	$3x10^{-5}$ to $3x10^{-2}$

In general, hafnium carbide-dispersed WHfC wires show a higher fracture ductility both at 1400 K (Fig. 6(a)) and 1600 K (Fig. 6(b)) than either the bubble-dispersed 218CS-W or the thoria-dispersed ST300-W. The ductility of WHfC is nearly constant --about 70 percent-- whereas that of 218CS and ST300-W at both 1400 and 1600 K drops from about 60 percent to 5 percent as the strain rate decreases.

Microstructure of Tested Wires

The microstructure of longitudinal sections and the fracture morphology of ST300-W wire after testing at 1600 K are shown in Fig. 7. Clearly, the fracture mode is dependent on deformation rate since essentially no necking was observed after slow straining (Fig. 7(a)); significant necking in the failure area was found after fast strain rate testing (Fig. 7(c)). Instead of failing by plastic flow, the slowly deformed samples apparently failed by the formation and growth of surface cracks along grain boundaries, with the general direction of the cracks being perpendicular to the tensile stress axis. Although the initial substructure of ST300-W (Fig. 1(b)) has been maintained in the high strain rate specimen (Fig. 7(d)), it has been segmented into 4- to 15-μm lengths, and its width has significantly increased after slow testing (Fig. 7(b)). The fracture behavior of ST300-W at 1400 K was identical to that observed at 1600 K. The WHfC fractures after fast and slow straining at either 1400 or 1600 K were analogous to those found after fast testing of ST300-W (Fig. 7(c)). The post-test microstructure of 218CS-W exhibited effects of strain rates on the fracture characteristics similar to those of ST300-W.

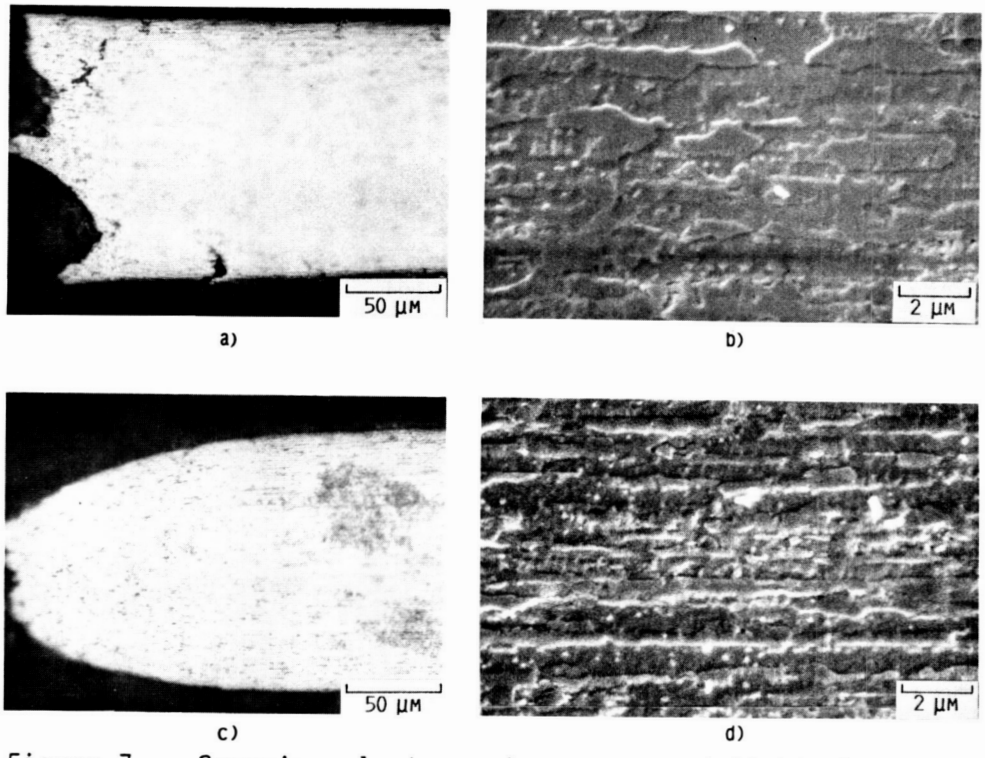

Figure 7. - Scanning electron microscope and light photomicrographs of ST300-W wires tested at 1600 K and a strain rate of 0.000033 sec^{-1} a) fracture region and b) away from fracture; and at a strain rate of 0.033 sec^{-1} c) fracture region and d) away from fracture.

By utilizing an intersection method (lines perpendicular to the wire axis), the width of the fibrous grain structure t was determined. For each condition, nearly 200 measurements were made at a distance about 1 mm from the fracture surface. Figure 8 illustrates the relative frequency of t as a function of strain rate for ST300-W and WHfC tested at 1600 K. Clearly, the

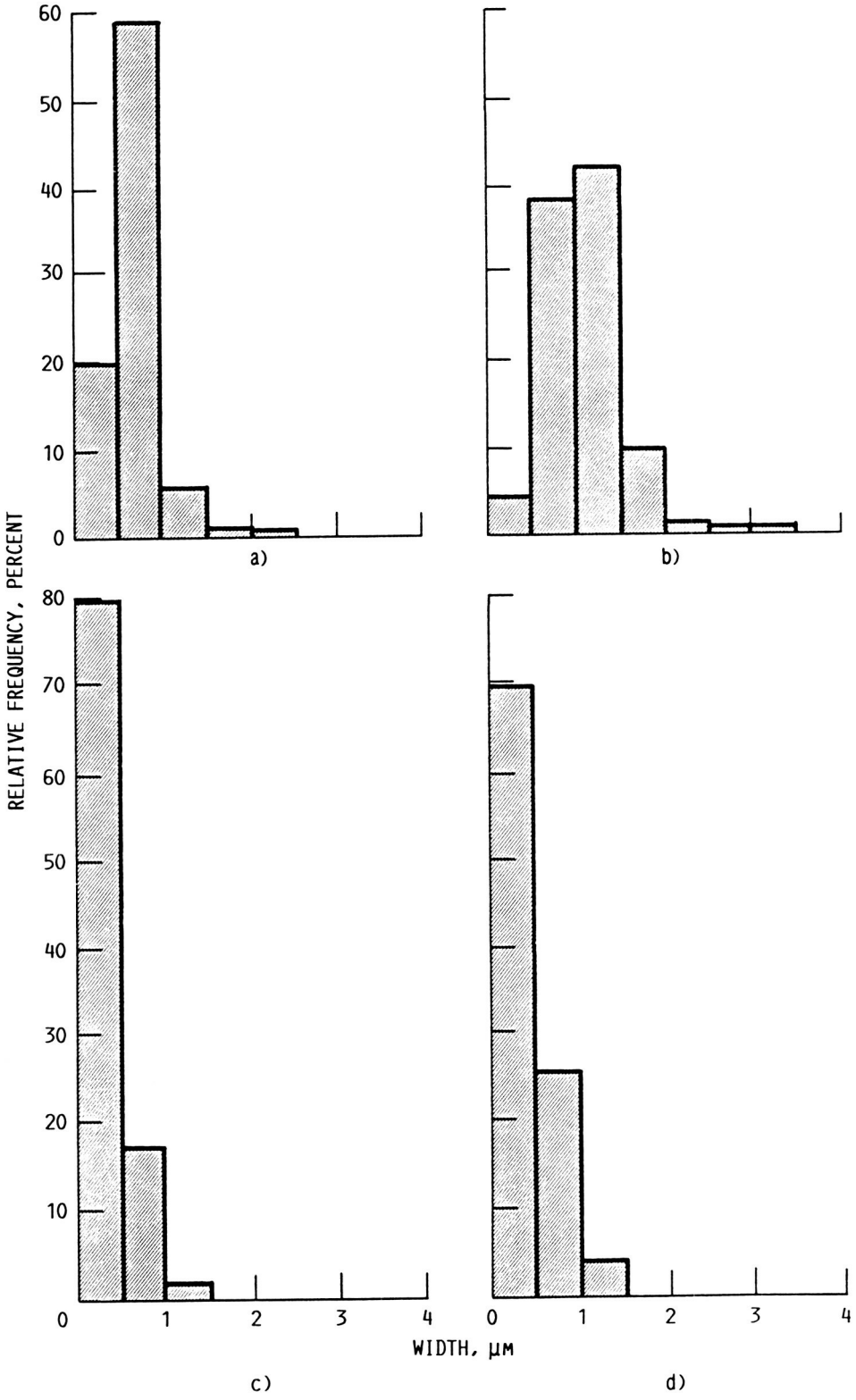

Figure 8. - Distribution of the fibrous substructure width, t, as a function of strain rate tested at 1600 K: a) 3.3×10^{-2} sec^{-1} for ST300-W, b) 3.3×10^{-5} sec^{-1} for ST-300-W, c) 3.3×10^{-2} sec^{-1} for WHfC, and d) 3.3×10^{-5} sec^{-1} for WHfC.

average grain width of ST300-W increased with decreasing strain rate (the median value of **t** was shifted from the 0.5 to 1.0 μm range to the 1.0 to 1.5 μm range). However, the median value of **t** for WHfC was unchanged under the same conditions. Since these microstructural observations can be correlated with the relationship between ductility and strain rate (Fig. 6(b)), losses in ductility might stem from microstructural instabilities owing to the original substructure being replaced due to drawing during the tensile tests.

Discussion

Strengthening Mechanisms

The tensile strength of a material can be increased by introducing a dispersion of second particles and/or by cold working. For example, particles which impede the motion of dislocations increase the Orowan stress. For a given matrix, the type of particle and the average diameter have some influence on the Orowan stress; however, the major factor affecting its magnitude is particle spacing. Dislocation substructure formed by prior cold working, where the stored elastic energy, density of sessile dislocations, and the average diameter of the subgrains affect strength, also impedes the movement of mobile dislocations. By utilizing data from the literature, the expected Orowan stresses for different dispersoids in the tungsten-alloy wires can be calculated and compared to the anticipated strengthening due to the retained fine substructure.

Strength Contribution via the Orowan Stress. The theoretical shear yield stress of dispersion-strengthened alloys has been calculated by Ashby (8). For a given second-phase diameter **d** and interplaner particle spacing distance **D**, the Orowan yield stress τ_O on the edge dislocations is directly proportional to the matrix shear modulus G_m (9); that is

$$\tau_O = (G_m b/2.36\pi D)\ln(d/2b) \qquad (3)$$

where **b** is the magnitude of the Burgers vector. With the assumption that the matrix chemistry is similar for all three wires, G_m and **b** are assumed to be identical for each system. Therefore, from previously measured values of **d** and **D** (4,10,11) (Table III), the Orowan stress for each type of wire can be calculated. For instance, at 1400 K τ_O equals 68 MPa for 218CS-W, 80 MPa for ST300-W, and 118 MPa for WHfC wires. The WHfC alloy is expected to be somewhat stronger than the others due to a higher Orowan stress.

Table III. - Characterization of the Dispersoids in the W-Alloy Wires

Dispersoid	Fiber	Average second-phase diameter, d, nm	Average interplaner particle distance, D, nm	Second-phase volume fraction, f, percent	Particle shear modulus, G_p,[a] G_m	Reference
Thoria	ST300-W	76	315	3.80	G_m	4
HfC	WHfC	35	180	1.55	G_m	10
Bubble	218CS-W	15	250	0.19	0.1 G_m	11

[a]In terms of G_m, the tungsten matrix shear modulus.

Substructure Strengthening. One contribution of the substructure to the yield stress results from the stored elastic energy, which can be considered to be a direct function of prior work-hardening. Such work-hardening is reported to be dependent upon the volume fraction of the second-phase **f** (8,12) as well as the accumulated plastic shear strain **a** (12). Work-hardening, derived from the dispersed second phase, is a result

of interactions between moving dislocations and particles according to Ashby (8). Thus the strengthening due to work-hardening Γ_{WH} is proportional to the root of the accumulated plastic strain,

$$\Gamma_{WH} = 0.24G_m\sqrt{bfa/d} \qquad (4)$$

Unfortunately the value of **a** cannot be determined presently because it is a direct function of the complicated and undefined fabrication schedules for each type of wire. If it is assumed that during production the original 10-μm grain diameter is reduced to 0.2 μm, the plastic shear strain would be 15.6 $--2\ell n(10/0.2)^2--$ and the shear stresses required for further deformation would be

$$\Gamma_{WH} = 343 \text{ MPa for 218CS-W}$$
$$\Gamma_{WH} = 1530 \text{ MPa for ST300-W}$$
$$\Gamma_{WH} = 1386 \text{ MPa for WHfC}$$

These values are most likely overestimates as some recovery occurs during process anneals which are part of wire fabrication schedules. The thoria- and HfC-strengthened materials should be much stronger than the potassium bubble-dispersed alloy. The work-hardening in a second-phase-strengthened alloy is estimated by Brown et al. (13) by a mean internal stress σ_M, which is proportional to the accumulated plastic strain in the matrix;

$$\sigma_M = 2Ka(G_pG_mf)/[G_p - K(G_p - G_m)] \qquad (5)$$

where **K** is a constant, ranging from 0.5 to 0.78 (14) depending on the accommodation between the matrix and particle. The required shear stress can be calculated if we assume that G_p is the particle shear modulus, that $G_p = G_m$ for thoria and hafnium carbide, and that $G_p = 0.1G_m$ for bubbles.

Calculated Orowan stresses and substructure strengths, normalized with respect to shear modulus of the matrix, are summarized in Table IV. For computations utilizing either Ashby's or Brown's model, three different values of the accumulated plastic shear strain were assumed: **a** = 0.1, 0.5 and 15.6. With the exception of the bubble-strengthened alloy, the Orowan stresses are generally small in comparison to the strength due to prior work. Clearly, Brown's substructure model indicates large differences in strength between bubble- and particle-hardened tungsten alloys, whereas Ashby's model is much less sensitive to the type of second-phase particle. For either model the strengths of the HfC or thoria alloys are similar; Brown's expression, however, leads to greater strengths than Ashby's.

Table IV. - Expected Orowan Stress Due to Dispersoids and Substructure Stress Due to Prior Working

Material	Orowan-to-matrix stress,[a] Γ_O/Γ_m	Work-hardening-to-matrix stress,[b] Γ_{WH}/Γ_m, 10^{-4}						Orowan-to-work-hardening stress,[b] Γ_O/Γ_{WH}	
		a = 0.1		a = 0.5		a = 15.6		a = 0.5	
		Eq. 4	Eq. 5	Eq. 4	Eq. 5	Eq. 4	Eq. 5	Eq. 4	Eq. 5
218CS-W	4.89×10^{-4}	4.47	1.27	10	6.3	55.8	198	0.33	0.44
ST300-W	5.78	8.91	38	19.9	190	111	5930	0.23	0.03
WHfC	8.53	8.36	15.5	18.7	77.5	104	2420	0.31	0.10

[a]From Eq. (3).
[b]For various a, accumulated plastic shear strain, mm/mm.

Figure 9 compares the measured to the estimated theoretical shear yield stress as functions of temperature and accumulated plastic shear strain. In this plot both shear strengths have been normalized with respect to shear modulus for tungsten where the experimental data were taken at a shear strain rate of 6.6×10^{-4} sec^{-1}. The theoretical values were based on a superposition of each strengthening mechanism where

$$\Gamma_{tot} = \Gamma_O + \Gamma_{WH} + \Gamma_m \tag{6}$$

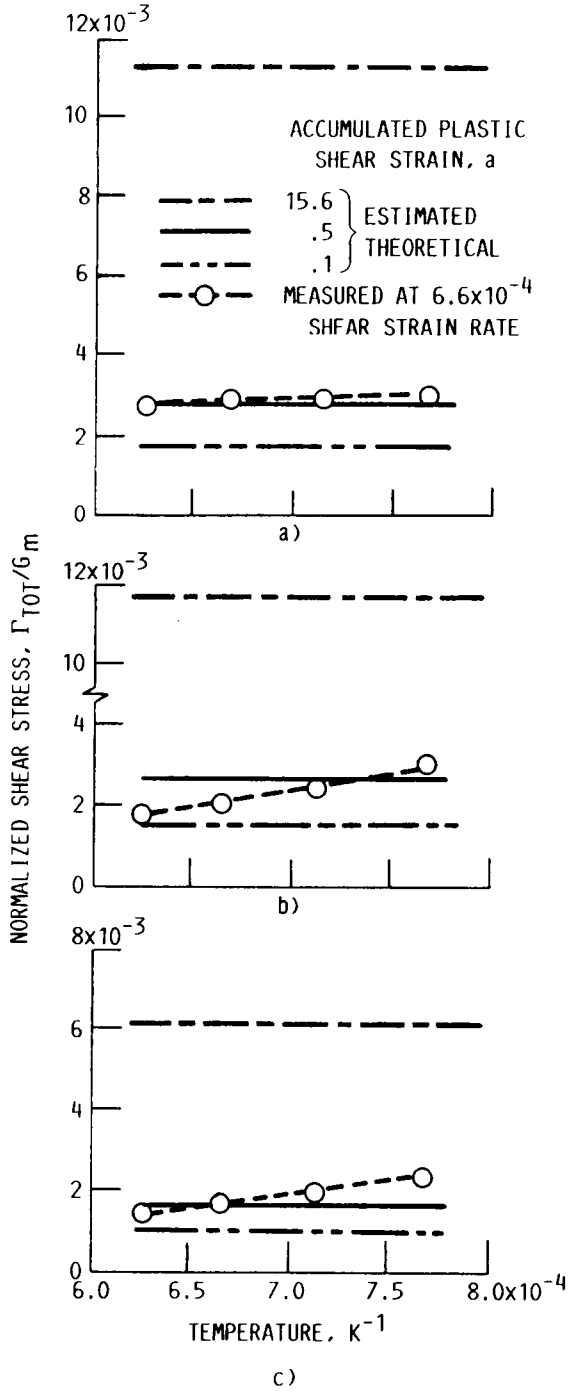

Figure 9. - Effect of temperature and prior work on theoretical shear stress due to superposition of substructure free motion, Orowan stress, and work-hardening stress for a) WHfC, b) ST300-W, and c) 218CS-W.

The matrix shear stress Γ_m, which is considered to be identical for all three wires, was taken as the strength of tungsten in the substructure-free and equiaxed grain size condition. The theoretical substructure stress was estimated from the Ashby model (Eq. (4)) because this model is the least sensitive to the plastic shear strain value. The estimated shear stresses for the wires as a function of temperature are in good agreement with the experimental data (shear stress = PL/2), if **a** is assumed to be about 0.5 for both ST300-W and WHfC. For 218CS-W a higher **a** value might be required.

Stability of the Fibrous Structure

The sharply decreasing strength of ST300-W and 218CS-W at strain rates less than 10^{-4} sec^{-1} at 1400 K (Fig. 5(a)) and at 1600 K (Fig. 5(b)) could be due to lack of second-phase stability and concurrent loss of resistance to recrystallization. According to Snow (15), Davis (16), and Barna (17), primary static recrystallization to a polycrystalline structure occurs in the temperature range of 1300 to 1400 K in 0.2 to 10 hr and is accompanied by a loss of the preferred fiber texture and a decreased grain aspect ratio. Secondary recrystallization, on the other hand, typically takes place above 1600 K with the loss of the fibrous structure and the coarsening of the doped or alloyed tungsten grains. During hot tensile or creep test conditions these temperature/time parameters should be reduced since dynamic recrystallization is an easier process.

The inhibition of recrystallization by a second phase is attributed to particles impeding the motion of the recrystallization front (11,18). Recrystallization will take place if the driving force of the grain boundary mobility is larger than the inhibiting force. According to Warlimont et al. (18) the impeding stress P_i is dependent on the second-phase distribution;

$$P_i = (2\tau_B f_B/r) + (2\tau_{SB} f_{SB}/r) \tag{7}$$

where τ_B and τ_{SB} represent specific grain or subgrain boundary energy, f_B and f_{SB} are the volume fraction of second-phase particles intersected by a unit of grain or subgrain, and **r** is the radius of particles or bubbles.

The driving force for recrystallization P_d is a result of the existing grain and subgrain boundary structure;

$$P_d = (2\tau_B/X_B) + (2\tau_{SB}/X_{SB}) \tag{8}$$

where X_B and X_{SB} are grain diameter and subgrain spacing, respectively. By equating Eqs. (7) and (8), the critical radius to recrystallization is defined

$$r_c = (1.1X_B X_{SB} f_B)/(X_{SB} + 0.1X_B) \tag{9}$$

when it is assumed that $\tau_{SB} = 0.1\tau_B$ and $f_{SB} = f_B$ (11). The theoretical equilibrium state for the radius of second-phase particles can be obtained by using parameters from the literature (18) where $\tau_B = 1.08$ J/m^2, $\tau_{SB} = 0.1$ J/m^2, $X_B = 0.5$ μm, $X_{SB} = 0.15$ μm, and $f_B = 5\pi d^2/4D^2$ for a grain boundary mobility perpendicular to the fiber axis; thus

r_c, bubble = 6 nm
r_c, thoria = 90 nm
r_c, HfC = 60 nm

Since these critical radii are the thresholds to recrystallization, larger values prohibit recrystallization.

Comparing the calculated radii to measured parameters (Table III) reveals that the estimated critical radii of thoria and HfC are greater than the initial particle radii, whereas the estimated critical size for the potassium-filled bubbles is less than that for the as-received material. Hence, on the basis of this theoretical calculation, one would expect bubble-strengthened materials to undergo recrystallization rather easily, whereas both particle-strengthened alloys should be resistant to such phenomena. This would seemingly indicate that the HfC- and thoria-containing materials should possess mechanical properties with less temperature and time sensitivity. In general, this seems to be the case (see Figs. 3 and 4).

If particle growth takes place during elevated temperature exposure, it is probable that the grain boundaries could break free and recrystallization would take place. Thus it becomes a question of which type of second phase is more stable. Unfortunately, the basic information, such as solubility of the elements comprising the particles in the metal matrix, interfacial energy between particle and matrix, and diffusivity, is not known; hence computations based on simple models (i.e., Wagner (19)) cannot realistically be made. However, based on the current work (Figs. 4 and 5), HfC appears to be more resistant to recrystallization than thoria.

Summary of Results

The tensile properties of 200-μm lengths of 218CS-W, ST300-W, and WHfC wires were examined in the temperature range of 1300 to 1600 K, and the following results were obtained:

1. A stress relief at 1535 K for 1 hr did not affect the tensile strength or ductility of ST300-W.

2. Electropolishing of ST300-W significantly improved the proportional strength and ductility but not the ultimate tensile strength.

3. The hafnium carbide-dispersed alloy had significantly better tensile properties than either the thoria- (ST300) or potassium bubble- (218CS) strengthened materials.

4. Calculations indicate that hafnium carbide-dispersed (WHfC) wires should possess a higher Orowan stress and a stable fibrous substructure and, thus, have superior high temperature tensile properties.

5. Hafnium carbide-dispersed (WHfC) wires are less sensitive to strain rate than bubble- or thoria-dispersed wires.

Conclusions

From the current work it is concluded that using hafnium carbide-strengthened wires will lead to stronger metal matrix composites than those from either of the currently available commercial tungsten alloys. The properties of hafnium carbide wires can be further improved by electropolishing to remove surface defects prior to composite fabrication.

References

1. B. Harris and E.G. Ellison: Trans. ASM, 1966, vol. 59, pp. 744-754.

2. R. Warren and C-H. Anderson: Proc. 10th Plansee Seminar, Vol. 2, H.M. Ortner, ed., Metallwerk Plansee, Austria, 1981, pp. 243-246.

3. D.B. Snow: Met. Trans. A, 1979, vol. 10, pp. 815-821.

4. G.W. King: Trans. TMS-AIME, 1969, vol. 245, pp. 83-89.

5. L.J. Westfall, D.W. Petrasek, D.L. McDanels, and T.L. Grobstein: NASA TM-87248, National Aeronautics and Space Administration, Washington, DC, 1986.

6. L.H. Amra, L.F. Chamberlain, F.R. Adams, J.G. Tavernelli, and G.J. Polanka: NASA CR-72654, National Aeronautics and Space Administration, Washington, DC, 1970.

7. Behavior and Properties of Refractory Metals, T.E. Tietz and J.W. Wilson, eds., Stanford University Press, Stanford, CA, 1965, p. 295.

8. M.F. Ashby: in Oxide Dispersion Strengthening, G.S. Ansell, T.D. Cooper, and F.V. Lenel, eds., Science Publishers, New York, 1968, pp. 143-205.

9. P.E. Armstrong, and H.L. Brown: Trans. TMS-AIME, 1964, vol. 230, pp. 962-966.

10. G.W. King and D.W. Petrasek: NASA TM-79115, National Aeronautics and Space Administration, Washington, DC, 1979.

11. H.P. Stuewe: Met. Trans. A, 1986, vol. 17, pp. 1455-1459.

12. R. Ebeling, and M.F. Ashby: Philos. Mag., 1966, vol. 13, pp. 805-834.

13. L.M. Brown, and D.R. Clarke: Acta Metall., 1977, vol. 25, pp. 563-570.

14 L.M. Brown, and D.R. Clarke: Acta Metall., 1975, vol. 23, pp. 821-830.

15. D.B. Snow: Met. Trans. A, 1976, vol. 7, pp. 783-794.

16. G.L. Davis: Metallurgia, 1958, vol. 58, pp. 177-184.

17. A. Barna, I. Gaal, O. Geszti-Herkner, G. Radnoczi, and L. Uray: High Temp.-High Press., 1978, vol. 10, pp. 197-205.

18. H. Warlimont, G. Necker, and H. Schultz: Z. Metall., 1975, vol. 66, pp. 279-286.

19. A.U. Seybolt: in Oxide Dispersion Strengthening, G.S. Ansell, T.D. Cooper, and F.V. Lenel, eds., Science Publishers, New York, 1968, pp. 469-487.

NASA
National Aeronautics and Space Administration

Report Documentation Page

1. Report No.	2. Government Accession No.	3. Recipient's Catalog No.
NASA TM-101446 DOE/NASA/16310-7		

4. Title and Subtitle	5. Report Date
Tensile Behavior of Tungsten and Tungsten-Alloy Wires from 1300 to 1600 K	
	6. Performing Organization Code

7. Author(s)	8. Performing Organization Report No.
Hee Mann Yun	E-4552
	10. Work Unit No. 586-01-11

9. Performing Organization Name and Address	11. Contract or Grant No.
National Aeronautics and Space Administration Lewis Research Center Cleveland, Ohio 44135-3191	
	13. Type of Report and Period Covered Technical Memorandum

12. Sponsoring Agency Name and Address	14. Sponsoring Agency Code
U.S. Department of Energy Reactor Systems Development and Technology Washington, D.C. 20546-0001	

15 Supplementary Notes

Final Report. Prepared under Interagency Agreement DE-AI03-86SF16310. Hee Mann Yun, National Research Council—NASA Research Associate, NASA Lewis Research Center. Prepared for The Metallurgical Society Fall Meeting, cosponsored by The Metallurgical Society of AIME and the American Society for Metals, Chicago, Illinois, September 27-29, 1988.

16. Abstract

The tensile behavior of 200-μm-diameter tungsten lamp (218CS-W), tungsten + 1.0 atomic percent (a/o) thoria (ST300-W), and tungsten + 0.4 a/o hafnium carbide (WHfC) wires was determined over the temperature range 1300 to 1600 K at strain rates of 3.3×10^{-2} to 3.3×10^{-5} sec^{-1}. Although most tests were conducted on as-drawn materials, one series of tests was undertaken on ST300-W wires in four different conditions: as-drawn and vacuum annealed at 1535 K for 1 hr, with and without electropolishing. Whereas heat treatment had no effect on tensile properties, electropolishing significantly increased both the proportional limit and ductility, but not the ultimate tensile strength. Comparison of the behavior of the three alloys indicates that the HfC-dispersed material possesses superior tensile properties. Theoretical calculations indicate that the strength/ductility advantage of WHfC is due to the resistance to recrystallization imparted by the dispersoid.

17. Key Words (Suggested by Author(s))	18. Distribution Statement
Tensile behavior; Thoria; Carbides; 218CS; ST300-W; WHfC; Orowan stress	Unclassified – Unlimited Subject Category 26 DOE Category UC-25

19. Security Classif. (of this report)	20. Security Classif. (of this page)	21. No of pages	22. Price*
Unclassified	Unclassified	16	A03

*For sale by the National Technical Information Service, Springfield, Virginia 22161